Seismic behaviour of reinforced concrete structural walls. Applications in Eurocode 8

M. Fischinger, J. Mazars, Panagiotis Kotronis, P. Kante, T. Isakovic

▶ **To cite this version:**

M. Fischinger, J. Mazars, Panagiotis Kotronis, P. Kante, T. Isakovic. Seismic behaviour of reinforced concrete structural walls. Applications in Eurocode 8. Fib-Symposium, Concrete structures in seismic regions, May 2003, Athens, Greece. pp.204-205. ⟨hal-01008871⟩

HAL Id: hal-01008871

https://hal.science/hal-01008871v1

Submitted on 27 Jan 2026

HAL is a multi-disciplinary open access archive for the deposit and dissemination of scientific research documents, whether they are published or not. The documents may come from teaching and research institutions in France or abroad, or from public or private research centers.

L'archive ouverte pluridisciplinaire **HAL**, est destinée au dépôt et à la diffusion de documents scientifiques de niveau recherche, publiés ou non, émanant des établissements d'enseignement et de recherche français ou étrangers, des laboratoires publics ou privés.

HAL Authorization

SEISMIC BEHAVIOUR OF RC STRUCTURAL WALLS APPLICATIONS IN EUROCODE 8

Matej FISCHINGER[1] Jacky MAZARS[2] Panagiotis KOTRONIS[3] Peter KANTE[4] Tatjana ISAKOVIĆ[5]

[1] Professor, University of Ljubljana, FGG, IKPIR, Jamova 2, SI-1000, Ljubljana, Slovenia
[2] Professor, INPG L3S, Domaine Universitaire BP 53 38041 Grenoble cedex 9 France
[3] Post-doc, L3S, Domaine Universitaire BP 53 38041 Grenoble cedex 9 France
[4] Ph.D. student, University of Ljubljana, FGG, IKPIR, Jamova 2, SI-1000, Ljubljana, Slovenia
[5] Assist. Professor, University of Ljubljana, FGG, IKPIR, Jamova 2, SI-1000, Ljubljana, Slovenia

Keywords: RC walls, EC8, damage mechanics, simplified models, multilayered Timoshenko beam, multiple-vertical-line-element

1 INTRODUCTION

Buildings with RC structural walls have been frequently built in Europe. The inherent (over)strength and stiffness of structural walls, as well as specific mechanisms of energy dissipation contributed to good response during some major earthquakes. However, on the other hand the behaviour of heavily loaded structural walls near collapse is very complex and difficult to model and predict without numerical models, specifically adapted for walls. Nevertheless, the research of the seismic response of structural walls has been rather limited in comparison with the frame structures. This also reflects in Eurocode 8 (EC8). The code, which is to a certain extent based on the studies of heavily loaded walls in the US and New Zealand, may not always address some European structural systems with the typically high wall-to-floor ratio. To solve this problem, additional experimental and analytical work is needed.

The home-Institutions of the authors have cooperated in a related action – CAMUS 3, which was the benchmark study of the shaking table response of a cantilever wall designed according to the EC8. CAMUS 3 was a part of several experimental campaigns on reinforced concrete bearing walls under seismic loading, which have taken place in France in the framework of French and European research programmes [1, 2, 3, 4]. These works were devoted mainly to the study of the in plane seismic behaviour of reinforced concrete bearing walls. CAMUS 3 experiment was a part of the 5th Topic “Shear Wall Structures” of the European program ICONS - TMR (Innovative Seismic Design Concepts for New and Existing Structures - Training and Mobility of Researchers) and of ECOEST2 (European Consortium of Earthquake Shaking Tables), [3]. The specimen was subjected to a series of 4 subsequent accelerograms on the Azalée shaking table of the EMSI Laboratory at CEA Saclay [4]. Blind prediction and post-experiment analyses were made by the benchmark participants. This was an opportunity to check the ability of the existing numerical models and related computer codes.

Nonlinear dynamic analysis of complex civil engineering structures based on a detailed finite element model requires large-scale computations and handles delicate solution techniques. The need for practical applicability and the stochastic nature of the input accelerations impose simplified numerical modeling that reduces computational cost. One way to proceed to a simplified 2D numerical analysis is to choose the classical Timoshenko beam theory to describe the global behaviour of the structural components. Beams are divided in several layers where simple biaxial or uniaxial constitutive relationships are used, sufficiently general though to take into account all the different inelastic phenomena. The French team used this model. The Slovenian team chose the multiple-vertical-line element model (MVLEM) macro model, originally proposed by Japanese researchers [5] and further modified and developed at the University of Ljubljana [6].

Using the chosen models, blind predictions were made in advance to the CAMUS 3 tests. Detailed analyses and further calibrations were made after the tests. Experimental and analytical evidence about the wall, designed according to EC8 was obtained.

2 CAMUS 3 TEST

2.1 Specimen description

The 1/3rd scaled CAMUS 3 model consisted of two parallel cantilever RC walls without openings linked by RC floors. The reinforcement was designed according to the EC8 design and detailing rules (Figures 1 and 2).

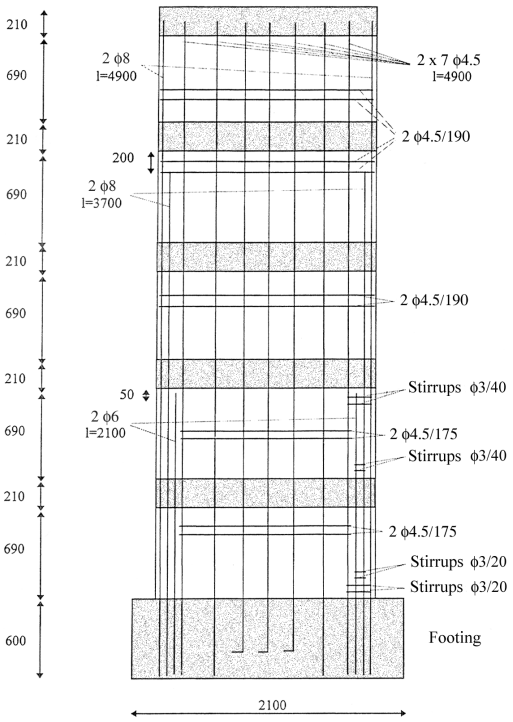

Fig. 1, Reinforcement – front view (in millimeters).

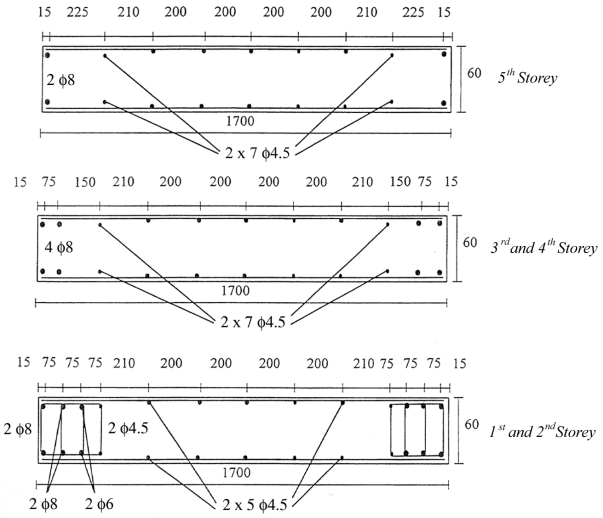

Fig. 2, Reinforcement – cross section (in millimeters).

Measured steel characteristics are given in Table 1.

Table 1 Measured steel characteristics

Diameter Φ (mm)	Type	Yield stress (MPa)	Rapture stress (MPa)	Ultimate strain (‰)
3.0	High adherence	814	849	14.5
4.5	High adherence	563	581	21.8
5.0	High adherence	631	646	9.3
6.0	High adherence	593	625	33.8
8.0	High adherence	486	587	168.0

It is important to note that the 3.0 mm to 6.0 mm bars show a high strength but very low ultimate strain, while 8.0 mm bars exhibit large ultimate strain. Compressive strength of the concrete was 39.6 MPa and Young modulus E = 31139 MPa.

2.2 Loading program

The generated accelerogram “Nice” was used as main input signal (Figure 3). An intermediate test was performed with the Melendy Ranch accelerogram (Figure 4). This signal has represented a “near-field earthquake”. This is short signal, but it has high value of acceleration and its frequency content corresponds to the natural frequency of the CAMUS 3 specimen ($T_{1,ini}$ = 0.155 s; Figure 5).

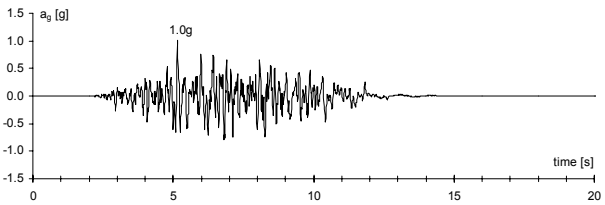

Fig. 3, Accelerogram Nice 1.00 g

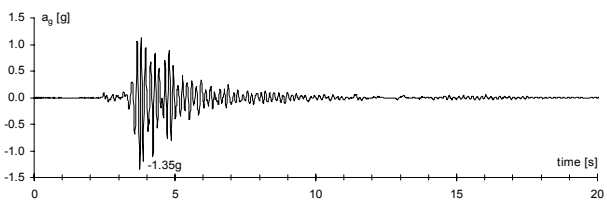

Fig. 4, Accelerogram Melendy Ranch 1.35g

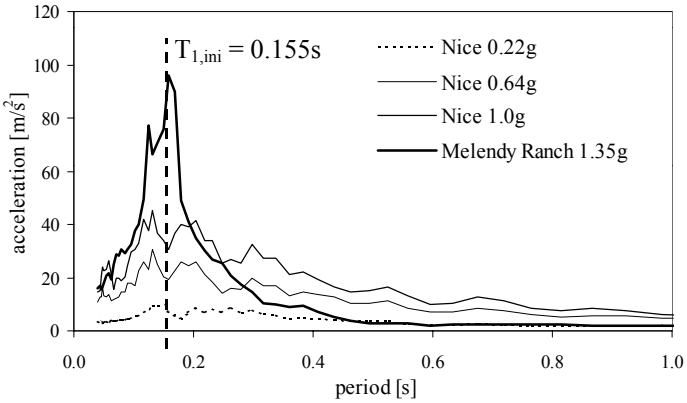

Fig. 5, Acceleration spectra for 2% of damping

Acceleration histories used in the analyses were measured on the shaking table. Maximum accelerations for the main tests (with the acceleration greater than 0.1g) are given in Table 2.

Table 2 Maximum acceleration of the table for the main seismic tests

Test	Nice	Nice	Melendy Ranch	Nice	Nice
Acceleration	0.42 g	0.22 g	1.35 g	0.64 g	1.0 g

For better understanding of the results and their application to EC8, it important to note that due to the problems in the control of the shaking table:

- Relatively strong accelerogram Nice 0.42g was applied at the very beginning of the loading program before the Nice 0.22g, which was supposed to be the first.
- Melendy Ranch 1.35g, was originally planned much weaker (0.90g). In fact it was 50% stronger, resulting in the application of the near collapse earthquake in the middle of the testing program (note again that the initial period of the specimen was close to the extreme peak in the spectrum – Figure 5).

2.3 Summary of the CAMUS 3 experimental results

The EC-8 designed wall behaved well (see section 5.3 for more details).

Other important observations include:

- The wall was already pre-cracked before the first test. The wall was further damaged by the unintended Nice 0.42g loading. There was no visible damage after this loading. There was also no much change in the natural frequency (from 6.88 to 6.44 Hz). However, the frequency that corresponded to the peak of the spectrum of the measured signal, changed much more.
- The Melendy Ranch seismic input motion caused important damage to the mock-up with extensive cracking and beginning of crushing at the wall extremities. Permanent displacements were observed at the end of the sequence, sign of residual cracks and significant yielding of the reinforcement bars. A large crack appeared throughout the base of each wall.
- After the Melendy Ranch seismic input motion, the strain gages situated just above the level of the construction joint of the first floor of the CAMUS 3 specimen indicated high strain values at this level on the one hand, and much lower values at the level corresponding to the 2nd and 3rd floor, on the other hand. Consequently damage seemed to be concentrated at the level of first story with large plastic rotation at the base. This fact was confirmed by the inspection of the specimen after the failure test (Nice S1 - 1.0g): almost all the vertical steel reinforcement bars were broken and buckled just above the level of the 1st construction joint. The zone where rupture of the bars took place followed the main cracks at the base (Figure 6).
- The displacement transducer at the top 6th storey (height: 5m) gave few reliable results. All analysis relevant to the top storey displacements in this paper refer to the 5th storey (height: 4.1m) results.
- Relative deflection (displacement vs. height) at the time of the collapse (Nice 1.0g) was about 1%.
- Ultimate bending capacity about 420 kNm was designed. The wall entered well into the inelastic range during the Melendy 1.35g loading (see also Chapter 4). Higher value, reached during the response (510 kNm) can be explained by the influence of the varying axial force.

- Significant axial force variations appeared at the medium and high level accelerations. The weight was sometimes doubled or reduced to zero. Even a net tension was observed during the Melendy 1.35g test.

Fig. 6, Specimen at the End of the Test (Right Wall)

3 NUMERICAL MODELS

3.1 2D multilayered Timoshenko beam elements and advanced local constitutive laws

In order to limit the model complexity (and resulting computational costs) structures are idealized using 2D multilayered Timoshenko beam elements and concentrated masses at specific points [7]. 1D or 2D constitutive laws are attributed at each layer and seismic loading is applied as an input motion at the base (Figure 7). Reinforcement bars are introduced within special composite layers whose behavior is obtained as a combination of those of concrete and steel according to:

$$\sigma_{layer} = (1 - a_{rel})\sigma_{concrete} + a_{rel}\sigma_{steel}\,, \tag{1}$$

where σ denotes axial stresses and α_{rel} is the relative area of the reinforcement in the layer.

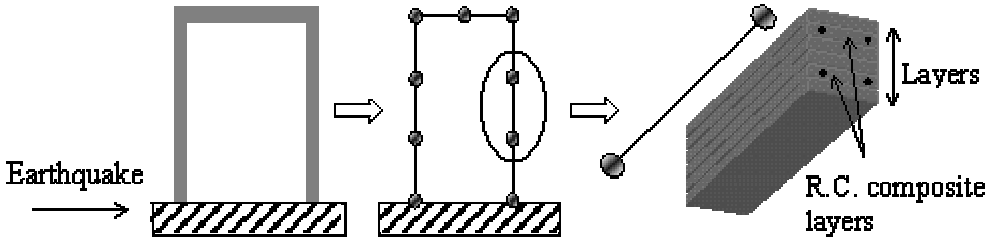

Fig. 7, Multilayered beam mesh for RC structures

Both steel and concrete are described within the thermodynamic framework for irreversible processes [8]. In describing the nonlinear behaviour of reinforcement bars, we choose the classical plasticity model and we take into account the nonlinear kinematic hardening of Armstrong and Frederick in order to be able to describe better the observed hysteretic loops [9]. A typical stress-strain hysteretic loop predicted by this model is given in Figure 8.

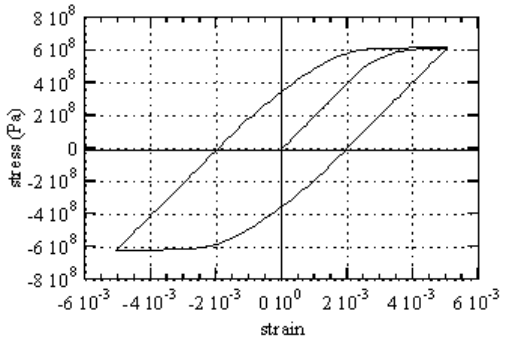

Fig. 8, Hysteretic Loop for Steel Modelling

The constitutive model for concrete under cyclic loading ought to take into account some observed phenomena, such as decrease in material stiffness due to cracking, stiffness recovery which occurs at crack closure and inelastic strains concomitant to damage. To simulate this behavior we use La Borderie's damage model that has two scalar damage variables, D_1 for damage in tension and D_2 for damage in compression [10]. Unilateral effect and stiffness recovery (damage deactivation) are also included. Inelastic strains are taken into account thanks to an isotropic tensor. The total strain is:

$$\boldsymbol{\varepsilon} = \boldsymbol{\varepsilon}^{\mathbf{e}} + \boldsymbol{\varepsilon}^{\mathbf{in}} \tag{2}$$

$$\boldsymbol{\varepsilon}^{\mathbf{e}} = \frac{\langle \boldsymbol{\sigma} \rangle_+}{E(1-D_1)} + \frac{\langle \boldsymbol{\sigma} \rangle_-}{E(1-D_2)} + \frac{\nu}{E}\left(\boldsymbol{\sigma} - Tr(\boldsymbol{\sigma})\boldsymbol{1}\right) \tag{3}$$

$$\boldsymbol{\varepsilon}^{\mathbf{in}} = \frac{\beta_1 D_1}{E(1-D_1)} \frac{\partial f(\boldsymbol{\sigma})}{\partial \boldsymbol{\sigma}} + \frac{\beta_2 D_2}{E(1-D_2)} \boldsymbol{1} \tag{4}$$

$\langle . \rangle_+$ denotes the positive part of a tensor. E is the initial Young's modulus and ν the Poisson ratio. β_1 and β_2 are material constants, $\boldsymbol{\varepsilon}^{\mathbf{e}}$ elastic strains and $\boldsymbol{\varepsilon}^{\mathbf{in}}$ inelastic strains, $\boldsymbol{1}$ denotes the unit tensor and $Tr(\boldsymbol{\sigma}) = \sigma_{ij}$ Damage criteria are expressed as $f_i = Y_i - Z_i$ ($i = 1$ for tension or 2 for compression, Y_i is the associated force to the damage variable D_i and Z_i a threshold dependent on the hardening variables) with $f(\boldsymbol{\sigma})$ the crack closure function. The evolution laws for the damage variables D_i are written as:

$$D_i = 1 - \frac{1}{1 + \left[A_i (Y_i - Y_{0i})\right]^{B_i}} \tag{5}$$

$$\begin{cases} Tr(\boldsymbol{\sigma}) \in [0, +\infty) & \rightarrow \dfrac{\partial f(\boldsymbol{\sigma})}{\partial \boldsymbol{\sigma}} = \boldsymbol{1} \\ Tr(\boldsymbol{\sigma}) \in [-\sigma_f, 0) & \rightarrow \dfrac{\partial f(\boldsymbol{\sigma})}{\partial \boldsymbol{\sigma}} = \left(1 - \dfrac{Tr(\boldsymbol{\sigma})}{\sigma_f}\right)\boldsymbol{1} \\ Tr(\boldsymbol{\sigma}) \in (-\infty, -\sigma_f) & \rightarrow \dfrac{\partial f(\boldsymbol{\sigma})}{\partial \boldsymbol{\sigma}} = 0.\boldsymbol{1} \end{cases} \tag{6}$$

Y_{0i} = initial elastic threshold ($Y_{0i} = Z_i(D_i = 0)$), σ_f the crack closure stress and A_i, B_i material constants. Figure 9 gives the stress-strain response of that model for a uniaxial traction-compression loading path.

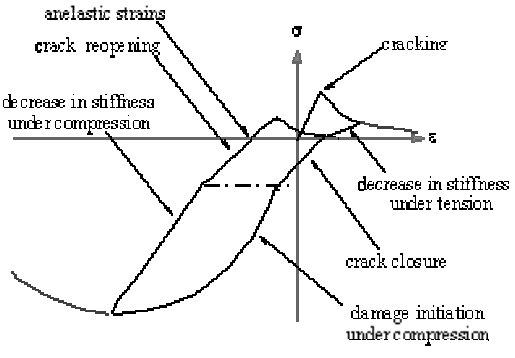

Fig. 9, Uniaxial response of concrete model subject to cyclic loading

Remark: When dealing with structures with a slenderness ratio far from the classical beam theory a more reliable representation of shear deformations and shear stresses has to be provided. One possibility in that respect – always within the family of simplified modeling strategies – is to use the Equivalent Reinforced Concrete model that privileges the use of lattice meshes for concrete and reinforcement bars [11, 12].

3.2 Multiple-vertical-line-element macro model (MVLEM)

Macro models consist of a finite number of discrete springs following certain force-displacement relationships, as opposed to stress-strain relationships in more detailed microelements. Macro elements attempt to describe the overall behaviour by means of an appropriate force-displacement idealisation. Multiple-vertical-line-element – MVLEM [13], incorporated into the well-known DRAIN-2D program, was used in CAMUS 3 benchmark (it was also successfully applied within the CAMUS 1 benchmark). In the model (Figure 10), several vertical springs are connected by rigid beams at the top and bottom level. They simulate axial and flexural behaviour of the wall segment (Figure 10 and 11a). Horizontal spring (Figure 11b) is modelling shear behaviour. Elastic shear behaviour was assumed in the final prediction for the benchmark study. More detailed description of the element is given in ✓5, 6☞.

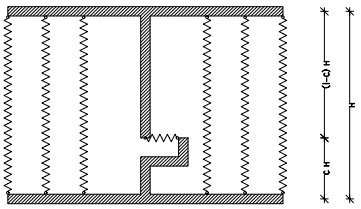

Fig. 10, Multiple-vertical-line-element model (MVLEM)

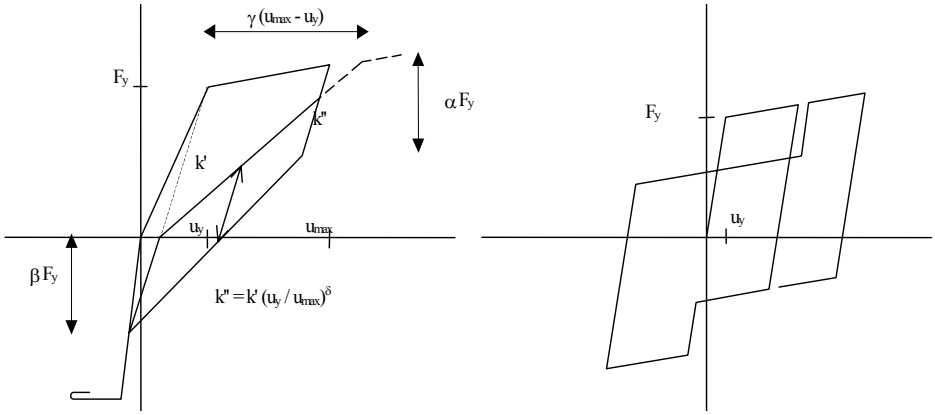

a) Vertical spring properties b) Horizontal spring properties

Fig.11, Spring properties

4 NUMERICAL SIMULATIONS

Simulations were carried out during both the pre- and post-experimental phases [3, 13, 14, 15].

4.1 Numerical simulations, using Timoshenko beam

The 2-D numerical model represents each wall as a cantilever beam whose behavior is controlled primarily by bending. Each wall is divided into 24 Timoshenko beam elements with 37 layers each. Concentrated masses are introduced at each floor. A single wall is considered (Figure 12). The horizontal bending beam was introduced to take into account the influence of the shaking table and the anchorage system. No calibration was made making the comparison with the experimental results presented hereafter similar to the one of a “blind simulation”.

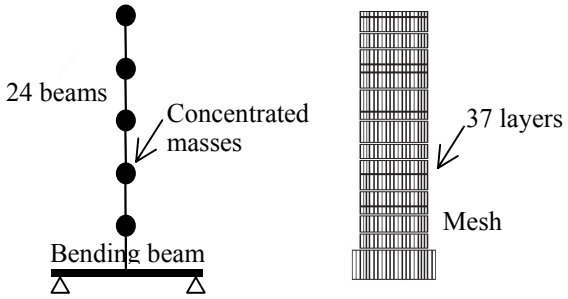

Fig.12, 2D numerical Model

Constitutive laws for concrete and steel are in 2D and 1D formulation respectively. Specific values for the materials are chosen according to the compressive, tensile and splitting tests (Table 3). The Young modulus of the base slab is taken smaller due to localized cracking already visible before the tests (those cracks appeared during the assembly of the specimens on the table particularly during the tightening of the wall anchorage to the floors). Bond slip and confinement are not taken into account. The damping coefficients have been adjusted to ensure a value of 2 % on the two first modes.

Table 3 Specific values used for the materials

Compression strength (concrete)	MPa	30
Tensile strength (concrete)	MPa	2.5
Young modulus (concrete)	MPa	30000
Young modulus at the base (concrete)	MPa	15000
Poisson coefficient (concrete)	-	0.2
Yield stress (steel)	MPa	414
Young modulus (steel)	MPa	200000

The modal analysis of the CAMUS 3 specimen shows that the numerical model is stiffer than the mock-up (7.25Hz predicted frequency for the first mode instead of 6.88Hz for the measured one). Due to an unreliable displacement transducer at the top of the specimen comparison of displacements is presented only at the fifth floor. Results of the simulation are compared with the experimental results in terms of displacements at the fifth floor and show a fairly good agreement (Figure 13).

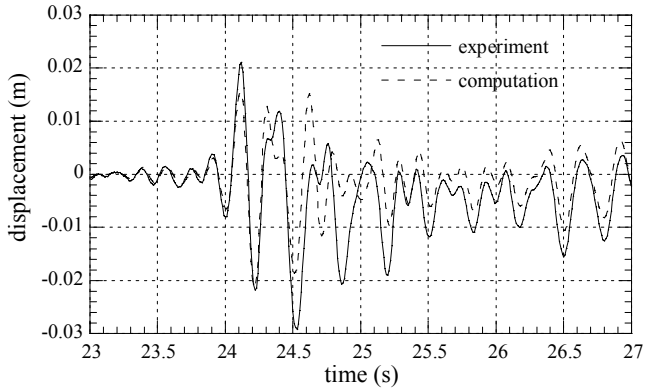

Fig. 13, Displacement Time History at the Fifth Floor (Melendy Ranch 1.35g)

Table 4 presents the comparison between model and experiment for the complete loading sequence. Results are satisfactory for the three first sequences. Significant differences however appear later on the displacements. Among possible reasons for this could be the fact that the model was more rigid than the specimen and bond slip was not taken into account.

Table 4 Global response comparisons

	Disp. fifth fl. (cm)		Shear force (kN)		Moment (kN.m)		Axial force (kN)	
	exp.	*comp.*	*exp.*	*comp.*	*exp.*	*comp.*	*exp.*	*comp.*
Nice S1 0.42g	0.7	0.6	79.6	78.8	263	247	222	232
Nice S1 0.24g	0.4	0.3	48.2	32.8	147	132	198	208
Mel. R 1.35g	2.9	2.1	151	153	510	469	374	348
Nice S1 0.64g	2.7	1.7	124	83.8	401	289	304	246
Nice S1 1.0g	4.7	2.4	140	123	410	364	314	292

Numerical and experimental results show a variation of the axial force at the base of the mock-up. As the cracks close, shock is induced, stiffness changes suddenly and the second mode (pumping mode) is excited [4, 16]. This variation of the vertical dynamic forces is important and for severe loading it can even double or cancel the axial force due to the dead weight of the specimen.

Experimentally, the phenomenon can be quantified by the measurement of an induced vertical acceleration at the shaking table. Figure 14 presents a sequence of the variation of the moment and

the dynamic variation of the axial force - referred to a zero initial value - of the CAMUS 3 specimen (computation). During the closure of the cracks (displacement or moment equal to zero) a higher compression appears suddenly. A tension force of the same order of magnitude immediately follows this dynamic axial compression.

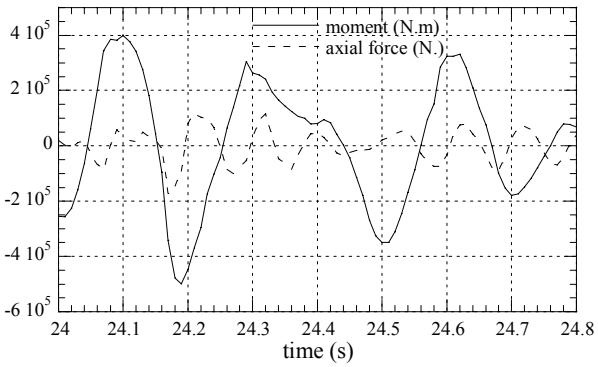

Fig. 14, Axial Force and Moment Time History

The damage variables D_1 and D_2 in Eq.(5) vary normally between 0 (non damaged section) and 1.0 (completely damaged section). By filtering their values between 0.95 and 1.0 we omit the micro-cracks and we have an image of the bigger cracks of the model. Figure 15 presents the damage pattern due to compression and tension at the end of the calculation for the complete loading program. Comparison with the actual position of cracks shows that again the model is able to reproduce the global trend observed experimentally (creation of the plastic zones at the base of the walls this time). The wall is mainly damaged at the base and that is in accordance with the EC8 design philosophy.

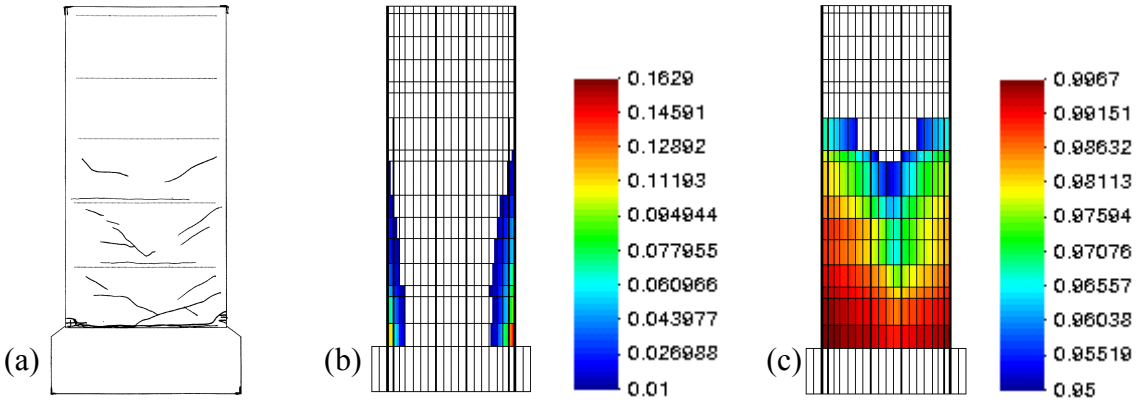

Fig. 15, Cracking of the Wall at the End of the Experiment (a)
Damage Pattern due to Compression (b) due to Tension (c).

4.2 Numerical simulations, using MVLEM model

First the comparison of the blind prediction and experimental results is given, following with the brief description of the post-experiment calibration. Low level (operational) and high level (near collapse) performance is studied separately.

4.2.1 Operational Performance

The correlation for the low level test Nice 0.22g is good, indicating that the model has been able to predict initial cracking and associated change in stiffness. Displacement time-history is presented in Figure 16 for illustration. Correlation coefficient is 0.78. If the preceding test Nice 0.42g was not taken into account, the results would be much poorer (correlation coefficient would be 0.15, only ; [13]).

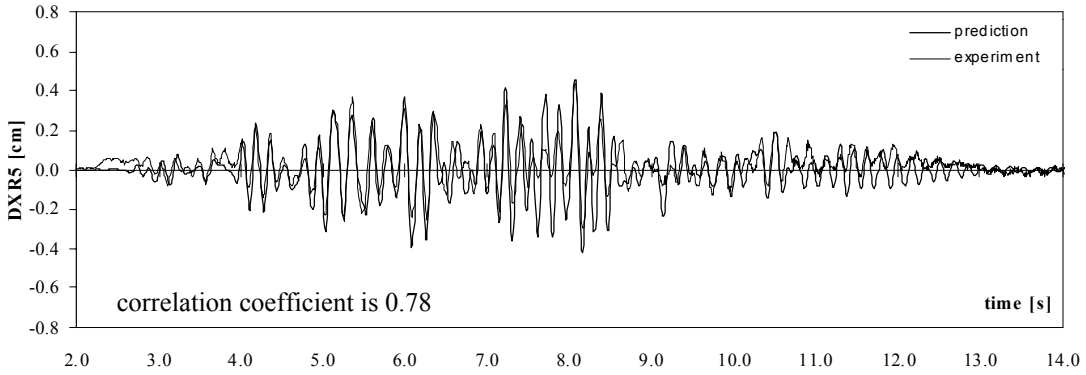

Fig.16, Displacement time-history: comparison of the predicted and experimental results (Nice 0.42g test was considered in the analysis)

4.2.2 Near Collapse Performance

Relatively simple analytical tool was also able to predict highly non-linear, but predominantly flexural response to Melendy Ranch signal (correlation coefficient was 0.65). However, this test was (unexpectedly) very strong. In addition to this, the structure and the loading were nearly in the perfect resonance and the damping was low. Consequently, accelerations of the specimen were nearly 10g (Figure 5), in comparison to the 0.75g design ground acceleration. It seemed that the wall was close to failure during the Melendy Ranch test. There has been some evidence that some reinforced bars were heavily damaged during this early test. Such heavily damaged specimen was subjected to two additional strong earthquakes. This actually changed the whole frame of the task. Such task would need elements and programs with the in-built failure criteria to monitor degradation of strength and even sudden drops of strength in the progressive collapse mechanism. Neither MVLEM nor DRAIN-2D has such options. Therefore it should be expected that the model could not predict substantial softening observed in the Nice 0.64g (Figure 17, correlation coefficient 0.44) and Nice 1.00g response (correlation coefficient 0.13!). Also the predictions in France and by majority of other benchmark participants, failed to simulate this softening.

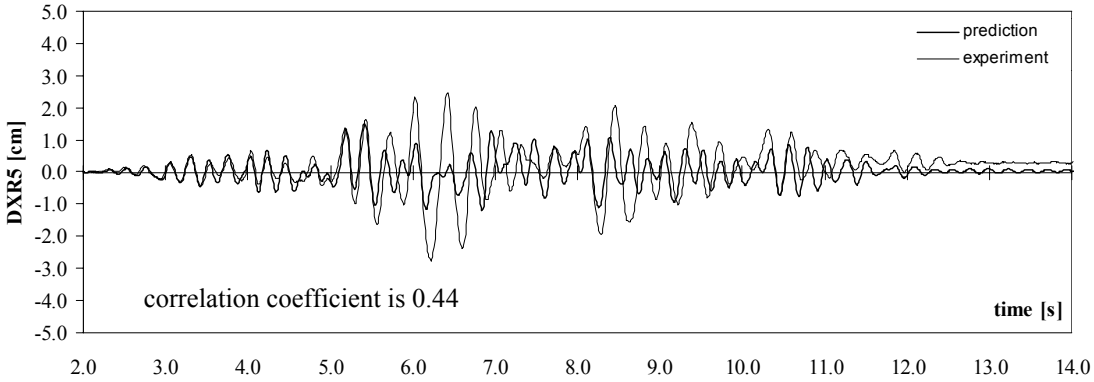

Fig.17, Displacement time-history /Nice 0.64g/. Softening of the wall was not predicted.

4.2.3 Correlation of the Analytical Prediction and Experimental Results

Table 5 Correlation coefficients between experimental and predicted results.

	Top disp. DXR5	Base shear TX1	Base moment MY1
Nice 0.22g	0.75	0.82	0.81
Melendy Ranch	0.66	0.63	0.67
Nice 0.64g	0.44	0.49	0.48
Nice 1.0g	0.13	0.26	0.23

4.2.4 Post-experiment calibrations

The following improvements of the numerical model were considered:

- It was supposed that some of the brittle reinforcement bars (Φ4.5 and Φ6) in the boundary columns were fractured during the Melendy Ranch test. Therefore they were excluded from the model during the subsequent Nice 0.64g and Nice 1.0g analyzes.
- The flexibility of the shaking table in the vertical direction was taken into account.
- Inelastic shear behaviour was assumed.

Results were considerably improved (compare Figures. 17 and 18 as well as Tables 5 and 6).

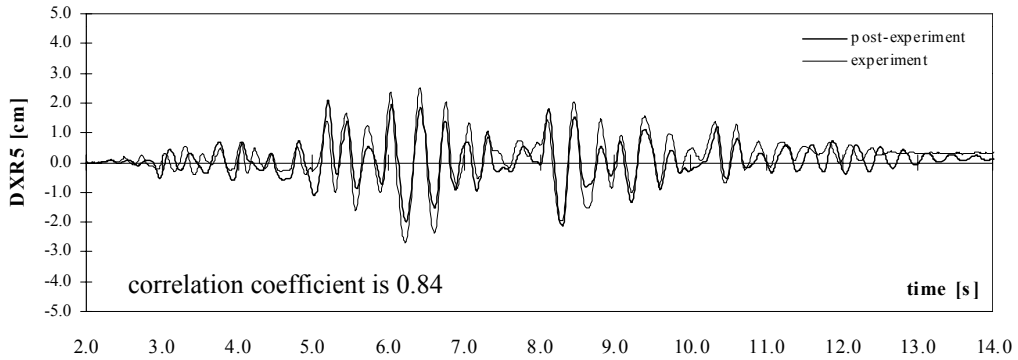

Fig.18, Displacement time-history /Nice 0.64g/ - improved model (compare with Figure 18)

Table 6 Correlation coefficients between experimental and post-experimental results

	Top disp. DXR5	Base shear TX1	Base moment MY1
Melendy Ranch	0.78	0.56	0.67
Nice 0.64g	0.84	0.80	0.81
Nice 1.0g			
[0 sec - 20.48 sec]	0.65	0.55	0.57
[5 sec - 8.5 sec]	0.87	0.71	0.75
[8.5 sec - 20.48 sec]	0.38	0.23	0.20

5 APPLICATIONS IN EC8

5.1 General

CAMUS 3 has not established clear relation between the model wall and actual prototype structures. Therefore the subsequent comments relate predominantly to the behaviour of the model. It is believed, however, that they can be generalized to the prototype structures.

5.2 Design

The reinforcement of the model (Figures 1 and 2) approximately corresponds to the design ground acceleration 0.75 g and behaviour factor q = 3 x 0.85 = 2.55. Reinforcement details have satisfied EC design practice and minimum reinforcement requirements. Overall percentage of vertical reinforcement is *0.4%.* Percentage of vertical reinforcement in boundary columns at the base is *2.1%.* Length of the boundary columns is *14%* of the length of the wall. Mechanical volumetric ratio of confining hoops within the critical region at the base is *0.4%.* Percentage of the distributed vertical reinforcement is *0.26%.* Percentage of the distributed horizontal reinforcement is *0.3%.*

The following values for bending moment resistance were calculated for the given reinforcement and design axial force due to vertical action (*N = 161 kN*): 283 kNm (design bending moment), 300 kNm (moment resistance calculated by design material characteristics; only reinforcement in boundary columns is taken into account), 365 kNm (all reinforcement is taken into account), 420 kNm (actual bending moment resistance).

The actual overstrength factor was 1.48. This overstrength influenced on the design shear force. The design shear at the base (88 kN) increased using capacity design procedure to 148 kN. Even if this increased value was taken into account, the resulting shear stress would be lower than *2 MPa*, which is a moderate value. The wall section with the provided shear reinforcement can resist this shear stress and flexural response can be expected.

5.3 Experimental evidence

The EC-8 designed wall behaved well in the frame of the foreseen mechanism:

- Capacity design worked as expected.
- Inelastic flexural deformations were confined to the first floor.
- Shear failure was precluded even in the case of severe loading.
- Confining of the edges of the wall was adequate to prevent failure up to the end of the test program.
- The wall survived much stronger loading than it was designed for.

Two additional important and less expected observations should be noted:

- Substantial varying axial force was induced into the cantilever wall due to its rocking response. This considerably influenced moment resistance as well as maximum induced shear force.
- The use of some brittle bars at the boundary columns nearly proved to be disastrous for the wall. There is evidence that short strong pulse of Melendey Ranch accelerogram brought these brittle bars almost to local failure (or debonding), substantially diminishing seismic capacity of the wall. Fortunately, most of the bars in the boundary columns were ductile. If not, the collapse would be difficult to avoid. This is a very serious warning in the time when the European market is flooded by cheap brittle reinforcement.

5.4 Parametric studies

Within CAMUS-3 the influence of the minimum reinforcement requirements on the eventual overstrength (which might be very important in the prototype structures) was not studied. Related parametric study is under way in the frame of the SAFERR project. Using MVLEM, hundreds of pushover analyses were made on cantilever walls representing actual structures with structural walls in Slovenia (height: 5 and 10 stories; wall-to-floor ratio: 1-4%; maximum ground acceleration: 0.1-0.3g). The study is not completed and the results have not been published yet. However, some important conclusions have been already made.

Most analysed walls representing actual structures possess large overstrength even in the case of the minimum EC8 reinforcement. Consequently, the response of low structures is practically elastic (with low ductility demand) in most cases. The same is valid for all buildings in areas with lower seismicity (ground acceleration 0.1 g). However, the demand increases rapidly in the case of 10-story buildings in higher seismicity areas. In this case the most important parameter proves to be wall-to-floor ratio.

This suggests that in the latter case the strict EC8 details for structural walls, which assure ductile behaviour as observed in the CAMUS 3 test, are needed. However, there are many other cases, when even minimum EC8 reinforcement provides such (over)strength that ductile structural details are not really needed. Precise definition of such cases is still not given.

6 CONCLUSIONS

6.1 Conclusions regarding EC8 design

CAMUS 3 research proved the efficiency of the EC8 design and detailing requirements. The wall behaved as foreseen by capacity design. Shear failure was precluded, damage was confined to the base, and confinement maintained integrity of the edges even in the case of very severe loading. In fact the wall resisted the loading considerably higher than expected in design.

Both, the capacity of the wall and the demand were high in comparison with the normal situation in western and central Europe. In the case of weak to moderate earthquakes, the overstrength due to minimum EC8 reinforcement is important. Parallel study in the frame of the SAFERR has demonstrated nearly elastic response of typical Slovenian structures in the case of lower buildings (5 story) as well as all buildings in low seismicity areas (maximum ground acceleration 0.1g). In addition to that the favourable effect of rocking on the dynamic behaviour of the structures was highlighted. The tests also demonstrated that the walls had a “multifuse” type of behaviour with additional sources of energy dissipation. Consequently, there are a number of cases, where strict EC8 detailing for high ductility structural walls is not needed. However, if needed the demand is high and EC8 requirements are justified. Precise definition of such cases is still needed.

The research demonstrated that substantial varying axial force was induced into the cantilever wall due to its rocking response. This considerably influenced moment resistance as well as maximum induced shear force.

The use of some brittle bars at the boundary columns nearly proved to be disastrous for the wall in the middle of the testing program. Fortunately, most of the bars in the boundary columns were ductile.

If not, the collapse would be difficult to avoid. This is a very serious warning in the time when the European market is flooded by cheap brittle reinforcement.

6.2 Conclusions regarding numerical modelling

Relatively simple – beam and/or macro models proved to be efficient to simulate operational and life safe performance. However, near collapse performance during 2 strong earthquakes following unexpectedly strong Melendy Ranch test was not predicted successfully in advance. This was due to the fact, that the models did not automatically detect local deterioration of brittle reinforcement (although this could be done with close inspection of the results). Fortunately, such situation (the heavily damaged wall has not been repaired before the next very strong event) is not likely to occur.

It was also demonstrated that the wall model should be able to simulate varying axial force in the cantilever wall due to the elongation of the neutral axis during the rocking response.

REFERENCES

[1] Coin, A., Fouré, B., Mazars, J., Gantenbein, F. et al. Programme CASSBA, final report (contrat MRT n°90F01114) Paris. 1993.

[2] Mazars, J.: French advanced research on structural walls: An overview on recent seismic programs. Proceedings of the 11th European Conference on Earthquake Engineering, Invited Lectures, Paris, CD-ROM. 1998.

[3] CAFEEL-ECOEST/ICONS. Thematic report N.5. Shear Walls Structures. Editors J.M. Reynouard, M.N. Fardis, September, LNEC, Lisboa, Portugal. 2001.

[4] Combescure D. & Chaudat Th.: ICONS European program seismic tests on R/C bearing walls. CAMUS III specimen. Rapport DMT, SEMT/EMSI/RT/00-014/A, CEA Saclay. 2000.

[5] Kabeyasawa, T., Shiohara, H., Otani, S., Aoyama, H. Analysis of the full-scale seven-story reinforced concrete test structure. Journ. Of the fac. Of Eng., Univ. of Tokyo, pp. 431-478. 1983.

[6] Fischinger, M., Vidic, T., Fajfar, P. Non-linear seismic analysis of structural walls using the multiple-vertical-line-element model. In: "*Non-linear Seismic Analysis and Design of Reinforced Concrete Buildings",* Bled, Slovenia, Elsevier, (edited by Peter Fajfar and Helmut Krawinkler), pp.191-202, 1992.

[7] Dubé, J. Modélisation simplifiée et comportement visco-endommageable des structures en béton. Ph. D., E.N.S. Cachan. 1994.

[8] Lemaitre J. & Chaboche J.L. Mécanique des matériaux solides. 2nd ed., Editions DUNOD. 1996.

[9] Armstrong, P.J & Frederick, C.O. A Mathematical Representation of the Multiaxial Bauschinger Effect. G.E.G.B. Report RD/B/N 731. 1966.

[10] La Borderie, Ch. Phénomènes unilatéraux dans un matériau endommageable : modélisation et application à l'analyse de structures en béton. Ph. D., Univ. Paris VI. 1991.

[11] Mazars J., Kotronis P. & Davenne L. A new modelling strategy for the behaviour of shear walls under dynamic loading. Earthquake Engineering and Structural dynamics, volume 31, issue 4, pp 937-954. 2002

[12] Kotronis P., Mazars J. & Davenne L. The equivalent reinforced concrete model for simulating the behavior of shear walls under dynamic loading. Engineering Fracture Mechanics 70 (7-8) pp. 1085-1097. 2003.

[13] Fischinger,M., Isaković, T., & Kante P. "CAMUS 3" International Benchmark – Report on numerical modelling, blind prediction and post-experimental calibrations, University of Ljubljana, IKPIR Report EE – 1/02, 2002.

[14] Kotronis P. Cisaillement dynamique de murs en béton armé. Modèles simplifiés 2D et 3D. Ph. D., E.N.S. Cachan. 2000.

[15] Mazars J., Kotronis P. & Crémer C. Analyses of seismic behaviour of structural walls with various reinforcements and boundary conditions. 12th World Conference on Earthquake Engineering, CD refer. number 2370. 2000.

[16] Ragueneau F. & Mazars J. Damping and Boundary Conditions, Two Major Points for the Description of the Seismic Behaviour of R/C Structures, Proc. XIth ECEE-98, CD-ROM, eds Bisch P., Labbé P. & Pecker A., Paris - CNIT La Défense. 1998.